

Modeling of 2D Corona Discharge in Dry and Humid Air: Ionic Wind and Ozone Production

T. Khattara^{1,2}, J. -M. Orlac'h³, P. Guitton¹ and C O. Laux²

¹Teqoya, Villandraut, 33730, France

²Université Paris Saclay, Laboratoire EM2C, CentraleSupélec, Gif sur Yvette 91192, France

³Département of Aerodynamics, Aeroelasticity, Acoustics, ONERA, Châtillon 92322, France

Abstract: The present study is dedicated to the 2D steady state simulation of ionic wind and ozone produced by a DC corona discharge between two parallel wires in atmospheric pressure air. A simplified air kinetics model is used to simulate charged species and ionic wind velocity. A chemical kinetics model of ozone involving neutral species is proposed to predict the ozone distribution in dry and humid air.

Keywords: Plasma, Corona discharge, Ionic wind, Ozone production.

1. Introduction

Inhaled dust particles, airborne microorganisms and aeroallergens can cause adverse health effects such as asthma and allergic diseases [1]. Corona discharges can be used for air purification by electrostatic precipitation. The ions produced by corona discharge deposit into the particles and the charged particles can then be attracted to grounded surfaces, resulting in electrostatic deposition, thus purifying the indoor air.

Corona discharge in air is accompanied by the generation of toxic gases especially ozone. Many experimental studies have revealed the dependence of ozone production on the discharge polarity, current levels, electrode size, air temperature and relative humidity [2], [3]. This work presents a model to predict ozone and ionic wind production in corona discharges in dry and humid air.

2. Numerical Model

The computational domain ($10 \times 6 \text{ cm}^2$) for the two parallel cylindrical wire geometry is shown in Fig. 1. The two electrodes are 9.0 mm apart. The anode is 0.2 mm in diameter and is biased to a high positive voltage. The cathode is 2 mm in diameter and is connected to the ground. A structured quadrilateral mesh is used near the two electrodes, and an unstructured triangular mesh is used in the rest of the domain allowing a homogeneous growth of the meshes until the limits. A mesh convergence study is performed to obtain the optimal balance between accuracy and runtime. The present model is a continuation of the work of Bérard et al. [4], [5]

When the corona discharge is operated, the high electric field ionizes the gaseous species surrounding the thin electrode. In the corona region (i.e. in the vicinity of the thin electrode) electron impact ionisation dominates over electron attachment, while outside the corona region, electron attachment prevails. Under the effect of the electric field, positive ions drift towards the grounded electrode, resulting into flow movement via momentum transfer from the ions to the neutrals. The driving term in the momentum equation (4) is the Lorentz force expressed as the product of the electric field by the net charge density.

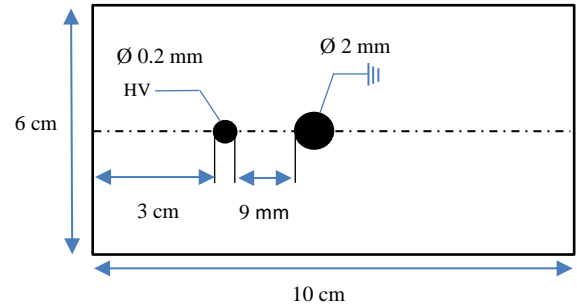


Fig. 1. Computational domain

The electric potential in the presence of charged species is calculated by the Poisson equation (1). The steady state drift-diffusion equations for electrons (2), positive and negative ions (3), neutrals (4) are solved simultaneously. Second order implicit scheme is used for all computations. Numerical simulations are made with the commercial software ANSYS Fluent CFD [6].

$$\Delta V = - \frac{e(n_+ - n_- - n_e)}{\epsilon_0} \quad (1)$$

$$\nabla \cdot (-\mu_e n_e \vec{E} - D_e \vec{\nabla} n_e) = S_e \quad (2)$$

$$\nabla \cdot (\pm \mu_{\pm} n_{\pm} \vec{E} - D_{\pm} \vec{\nabla} n_{\pm}) = S_{\pm} \quad (3)$$

$$\nabla \cdot (n_n \vec{u} - D_n \vec{\nabla} n_n) = S_n \quad (4)$$

$$\nabla \cdot (\rho \vec{u} \vec{u}) = -\vec{\nabla} P + e(n_+ - n_- - n_e) \vec{E} + \nabla \cdot \vec{\tau} \quad (5)$$

Where V and \vec{E} represent the electrical potential and the electric field, n_e, n_+, n_- and n_n are the densities of electrons, positive ions, negative ions and neutral species respectively. μ, D and S are the mobilities, diffusion coefficients and source terms of indicated species, \vec{u} is the bulk velocity of the fluid and $\vec{\tau}$ is the viscous stress tensor.

The chemical model in dry air involves electrons, one species of positive ions, one species of negative ions, the excited molecule $N_2(B)$ that contributes to the dissociation of oxygen molecules, and 7 neutral species ($O_2, N_2, O, N,$

O₃, NO, N₂O). The model considers 18 chemical reactions listed in Table 1. The rates of electron-impact reactions are recalculated at each iteration, as it depends on the electric field and electron density.

To study the effect of the relative humidity on ozone production, a list of chemical reactions involving H₂O related species are added. The additional chemical model contains 18 reactions and 7 species (H₂O, OH, H, HO₂, H₂O₂, HNO₂, HNO₃) as shown in Table 2. The prediction of the complete model have been compared - for different degrees of relative humidity - with other models proposed by Peyroux [7], Chen [2] and Sarrette [8]. Simulation of the temporal evolution of the relevant species studied were in good agreement. In this work, we assume that the formation of ozone in dry and humid air is not strongly influenced by excited and ionized species [7]. Additional charged species in particular water cluster ions, will be considered in future work to determine their influence on the formation of ozone in corona discharges.

Table 1. Chemical kinetics model for dry air, A⁺ stands for the generic positive ions (O₂⁺, N₂⁺). M is a third body.

No.	Reaction	Ref.
1	$e + A_2 \Rightarrow 2 e + A_2^+$	[4]
2	$e + O_2 \Rightarrow O^- + O$	[4]
3	$e + A_2^+ \Rightarrow A + A$	[4]
4	$A_2^+ + O^- \Rightarrow A_2 + O$	[4]
5	$O^- + M \Rightarrow e + O + M$	[4]
6	$e + N_2 \Rightarrow e + 2 N$	[9]
7	$e + O_2 \Rightarrow e + 2 O$	[9]
8	$e + O_3 \Rightarrow e + O + O_2$	[9]
9	$e + N_2 \Rightarrow N_2(B) + e$	[9]
10	$N_2(B) + O \Rightarrow NO + N$	[9]
11	$N_2(B) + O_2 \Rightarrow N_2 + 2 O$	[9]
12	$O + O_2 + O_2 \Rightarrow O_3 + O_2$	[9]
13	$O + O_2 + N_2 \Rightarrow O_3 + N_2$	[9]
14	$O_3 + O_2 \Rightarrow O + O_2 + O_2$	[10]
15	$O_3 + N_2 \Rightarrow O + O_2 + N_2$	[10]
16	$O_3 + O \Rightarrow O_2 + O_2$	[9]
17	$O_3 + NO \Rightarrow NO_2 + O_2$	[9]
18	$N + O_2 \Rightarrow NO + O$	[9]

The rates of ionisation and attachment, and the diffusion coefficients of electrons are fitted from Bolsig data for an air-like mixture [N₂]:[O₂] = 4:1 [5]. The mobility of electrons is taken from Chen et al. [11] as:

$$\mu_e = 1.2364E^{-0.2165} m^2V^{-1}s^{-1} \quad (6)$$

The mobilities of generic positive and negative ions are $\mu_+ = 2.5 \times 10^{-4} m^2/V/s$ and $\mu_- = 2.7 \times 10^{-4} m^2/V/s$ respectively, they are taken from Bérard et al [5]

Table 2. Additional reactions for humid air

No.	Reaction	Ref.
19	$e + H_2O \Rightarrow H + OH + e$	[7]
20	$O + OH \Rightarrow O_3 + H$	[7]
21	$OH + O_3 \Rightarrow HO_2 + O_2$	[7]
22	$2 OH \Rightarrow H_2O + O$	[7]
23	$2 OH + O_2 \Rightarrow H_2O_2 + O_2$	[7]
24	$2 OH + N_2 \Rightarrow H_2O_2 + N_2$	[7]
25	$OH + HO_2 \Rightarrow H_2O + O_2$	[7]
26	$H + O_2 + N_2 \Rightarrow HO_2 + N_2$	[7]
27	$H + O_3 \Rightarrow OH + O_2$	[7]
28	$H + HO_2 \Rightarrow 2 OH$	[7]
29	$N + OH \Rightarrow NO + H$	[7]
30	$NO + OH + N_2 \Rightarrow HNO_2 + N_2$	[7]
31	$NO + OH + O_2 \Rightarrow HNO_2 + O_2$	[7]
32	$NO + HO_2 \Rightarrow NO_2 + OH$	[7]
33	$NO_2 + OH + O_2 \Rightarrow HNO_3 + O_2$	[7]
34	$NO_2 + OH + N_2 \Rightarrow HNO_3 + N_2$	[7]
35	$HO_2 + NO_2 \Rightarrow HNO_2 + O_2$	[7]
36	$H_2O + O \Rightarrow 2 OH$	[7]

3. Results and Discussion

3.a) Charged species and ionic wind production:

Fig. 2 shows the density profiles of charged species along the inter-electrode line calculated at 9 kV. The electron density decreases rapidly away from the anode because ionization is the highest near the anode and because of dissociative attachment (R2). The number density of positive ions increases rapidly and reaches values much greater than the number densities of negative ions and electrons over most of the inter-electrode zone, leading to the creation of positive unipolar region between the two electrodes.

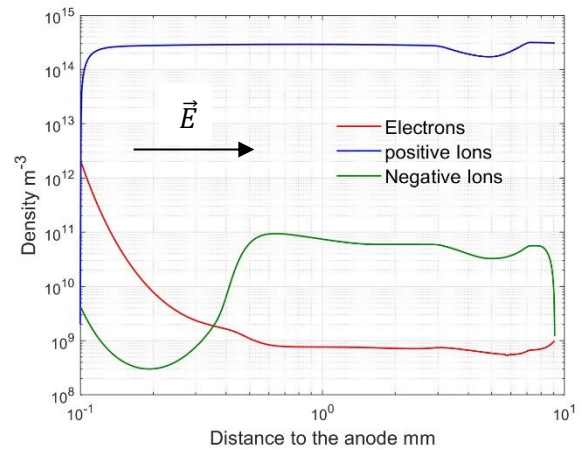


Fig. 2. Density of charged species along the inter-electrode gap, gap distance: 9 mm, anode voltage: 9 kV.

A comparison of the electric fields calculated in vacuum and in the presence of charges is shown in Fig. 3,

indicating that the charge density distribution presented in Fig. 2 induces a small distortion in the Laplacian field.

The one- and two-dimensional profiles of ionic wind velocity are plotted in Fig. 4. Between the two electrodes, velocity magnitude reaches 1.7 m/s as a maximum at an applied voltage of 12 kV. These results show that the present kinetics model can reproduce the increase in velocity induced by increasing the anode voltage. At high voltages, the values are relatively in accordance with measurements [5] with an estimated error less than 2%, while at 9 and 11 kV the calculated velocity is lower than the measured one, mainly due to the simplified kinetics model used for charged species.

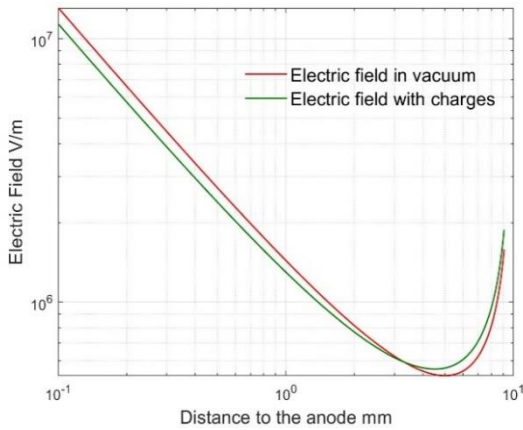


Fig. 3. Comparison of the electric field calculated in vacuum and with charged species.

3.b) Ozone production in dry and humid air:

The distribution of ozone density along the inter-electrode line in dry air and for different degrees of relative humidity are compared in Fig. 5. The rate of ozone production decreases with increasing relative humidity. As shown in Table 3, the ozone production rate decreases by more than 50% with RH = 10%.

Table 3. Effect of RH on ozone production rate

	Relative humidity			
	0 %	10 %	50 %	100 %
Ozone production rate [molecule/m ³ /s]	9.45e14	4.31e14	1.35e14	7.26e13
Decrease in ozone production rate [%]	0 %	54 %	86 %	92 %

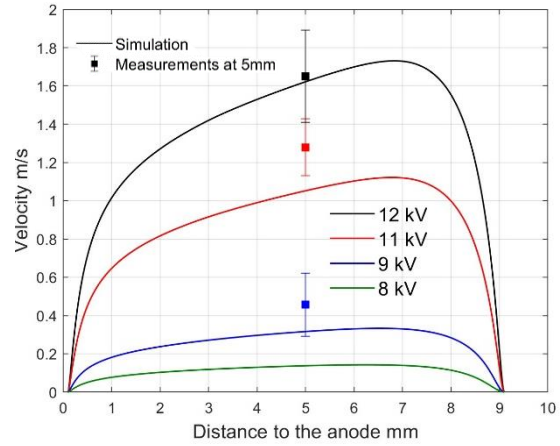
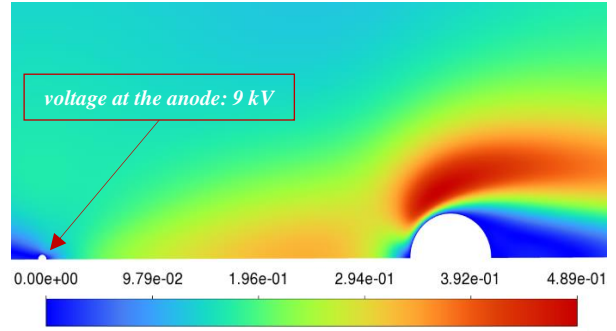


Fig. 4. a) Two-dimensional profile of ionic wind velocity. b) Ionic wind velocity profile along the inter-electrode gap at different voltages.

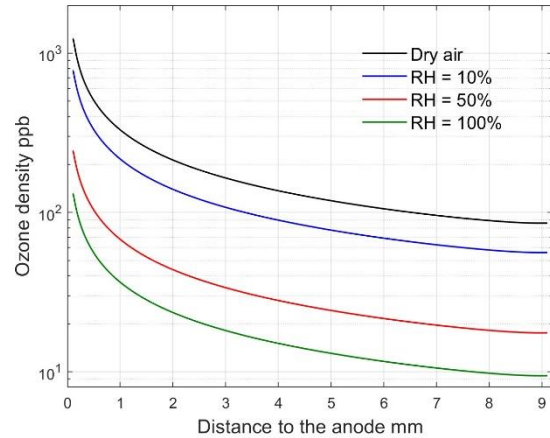


Fig. 5. Density of ozone along the inter-electrode gap in dry and humid air, gap distance: 9 mm, anode voltage: 9 kV.

4. Conclusion and perspectives

In this work, a numerical model is developed to simulate ionic wind velocity and ozone production by corona discharges in dry and humid air. The model solves Poisson equation and the drift-diffusion equations with plasma chemistry and transport phenomena. The kinetic model of ozone involves only neutral species. The effect of relative

humidity on the rate of ozone production is in agreement with other results [2], [7], [8]. The simulations will be extended to consider the ionized species that are created by the presence of water vapor in air (water cluster ions) to elucidate their influence on ionic wind and ozone production.

5. Acknowledgement

This work has been supported by a CIFRE Ph.D. grant (n° 2021/1779) from TEQOYA and the *Association Nationale de la Recherche et de la Technologie*.

6. References

[1] H. Burger, "Bioaerosols: Prevalence and health effects in the indoor environment," *Journal of Allergy and Clinical Immunology*, vol. 86, no. 5, pp. 687–701, Nov. 1990, doi: 10.1016/S0091-6749(05)80170-8.

[2] J. Chen and P. Wang, "Effect of relative humidity on electron distribution and ozone production by DC coronas in air," *IEEE Transactions on Plasma Science*, vol. 33, no. 2, pp. 808–812, Apr. 2005, doi: 10.1109/TPS.2005.844530.

[3] K. J. Boelter and J. H. Davidson, "Ozone Generation by Indoor Electrostatic Air Cleaners," *Aerosol Science and Technology*, vol. 27, no. 6, pp. 689–708, Jan. 1997, doi: 10.1080/02786829708965505.

[4] P. Bérard, D. Lacoste, and C. Laux, "Measurements and Simulations of the Ionic wind Produced by a DC Corona Discharge in Air, Helium and Argon," in *AIAA paper 2007-4611, 38th Plasmadynamics and Lasers Conference*, Miami, Florida, Jun. 2007. doi: 10.2514/6.2007-4611.

[5] P. Bérard, *Etude du vent ionique produit par décharge couronne à pression atmosphérique pour le contrôle d'écoulement aérodynamique*. Ph.D. thesis, Ecole Centrale Paris, 2008.

[6] "Ansys® Academic Research Mechanical, Version 21.1." [Online]. Available: <https://www.ansys.com/fr-fr>

[7] R. Peyrous, "The Effect of Relative Humidity on Ozone Production by Corona Discharge in Oxygen or Air – A Numerical Simulation – Part II : Air," *Ozone: Science & Engineering*, vol. 12, no. 1, pp. 41–64, Jan. 1990, doi: 10.1080/01919519008552454.

[8] J. P. Sarrette, O. Eichwald, F. Marchal, O. Ducasse, and M. Yousfi, "Electro-Hydrodynamics and Kinetic Modeling of Dry and Humid Air Flows Activated by Corona Discharges," *Plasma Sci. Technol.*, vol. 18, no. 5, pp. 469–472, May 2016, doi: 10.1088/1009-0630/18/5/04.

[9] I. A. Kossyi, A. Y. Kostinsky, A. A. Matveyev, and V. P. Silakov, "Kinetic scheme of the non-equilibrium discharge in nitrogen-oxygen mixtures," *Plasma Sources Sci. Technol.*, vol. 1, no. 3, pp. 207–220, Aug. 1992, doi: 10.1088/0963-0252/1/3/011.

[10] M. Capitelli, C. M. Ferreira, B. F. Gordiets, and A. I. Osipov, *Plasma Kinetics in Atmospheric Gases*. Springer Science & Business Media, 2013.

[11] J. Chen and J. H. Davidson, "Electron Density and Energy Distributions in the Positive DC Corona: Interpretation for Corona-Enhanced Chemical Reactions," *Plasma Chemistry and Plasma Processing*, vol. 22, no. 2, pp. 199–224, Jun. 2002, doi: 10.1023/A:1014851908545.